

Kagome-like lattice of π - π stacked 3-hydroxyphenalenone on Cu(111)[†]

Cite this: *Chem. Commun.*, 2014, 50, 8659

Received 9th May 2014,
Accepted 12th June 2014

DOI: 10.1039/c4cc03523b

www.rsc.org/chemcomm

S. Beniwal,^a S. Chen,^{bc} D. A. Kunkel,^a J. Hooper,^d S. Simpson,^e E. Zurek,^e
X. C. Zeng^{bc} and A. Enders^{*ac}

We have identified a structurally complex double-layer of 3-hydroxyphenalenone on Cu(111), which exhibits Kagome lattice symmetry. A key feature is the perpendicular attachment of π - π stacked molecular dimers on top of molecules that are flat-lying on the substrate, representing a rare example of a three-dimensional arrangement of molecules on a two-dimensional surface.

Crystalline structures of geometry corresponding to trihexagonal tiling are often referred to as Kagome lattices. Natural examples of Kagome lattices are rare, but have recently been found in surface supported organics.¹ Their particular geometry of interlacing triangles, exhibiting an ordered arrangement of hexagonal and triangular pores of different size, makes Kagome lattice structures exceptional templates for host-guest chemistry. Advances in surface science and the availability of high-resolution microscopy have accelerated the discovery of Kagome-lattice-type organic layers. Reported structures are typically based on van der Waals forces, hydrogen bonds or metal organic bonds.¹⁻³ Herein we report the first π - π stacked organic Kagome lattice, which consists of 3-hydroxyphenalenone (3-HPLN) molecules. A unique feature of the networks formed on flat Cu(111) is its three-dimensional architecture, which emerges from the perpendicular attachment of π - π stacked 3-HPLN dimers on planar, hydrogen-bonded molecular trimers.

3-HPLN is a topological, or proton transfer ferroelectric in its bulk crystalline form,¹¹ in which intermolecular hydrogen bonds couple to the molecular π electron systems and hence the molecular dipole moment, giving rise to a switchable polarization.⁴

Our team has recently discovered self-assembled chiral structures consisting of 3-HPLN trimers on Ag(111) surfaces,⁵ as well as complex 2D networks of the related molecular ferroelectrics croconic acid and rhodizonic acid.^{6,8} Several of these networks exhibit similar hydrogen bonds in their ferroelectric bulk phase, so there is reason to believe that ferroelectric order is possible in 2D structures as well.⁶ A few of the observed networks are porous, such as croconic acid on both Ag(111) and Au(111), and some structural phases of 3-HPLN on Ag,^{5,6} which can be attributed to interactions with the substrate as well as effective shape and entropy arguments.⁵

Driven by these findings, we investigated the self-assembly of 3-HPLN on Cu(111) substrates. Deposition of 3-HPLN at room temperature results in elongated islands, two or three molecules wide and several nanometers long, as seen in scanning tunneling microscopy (STM) images such as those presented in the ESI.[†] The molecule-to-molecule distance of 9.0 Å is consistent with molecules that are flat-lying on the surface, forming hydrogen bonds with one another. Post-annealing the sample to approximately 120 °C and higher results in the growth of the 2D islands due to Ostwald ripening. The arrangement of the molecules in those islands corresponds to hydrogen-bonded 1D chains as in the bulk,⁴ which form 2D islands likely through van der Waals attraction, as can be seen in Fig. 1a.

Only if the coverage of 3-HPLN is sufficiently high, exceeding two nominal layers, then similar post-annealing of the room-temperature-deposited molecules to 200 °C drastically changes the morphology of the film, as seen in Fig. 1b. We observe double layers of 3-HPLN consisting of two competing structures, a linear one and a honeycomb structure. Important structural details can be obtained from high-resolution STM images such as those in Fig. 1c-f. It appears that the molecules of the bottom layer, which are in direct contact with the substrate, are flat-lying on the surface, while the molecules in the top layer appear to be standing upright on the bottom layer, as is evident from their considerably smaller apparent size. While we were unable to fully resolve the molecular arrangement in the bottom layers, it is clear that it is different for the linear- and the honeycomb-like layers,

^a Department of Physics and Astronomy, University of Nebraska-Lincoln, 855 N 16th Street, Lincoln, NE, 68588-0299, USA. E-mail: aenders2@unl.edu; Fax: +1 402 472 6148

^b Department of Chemistry, University of Nebraska-Lincoln, NE, 68588, USA

^c Nebraska Center of Materials and Nanoscience, University of Nebraska-Lincoln, NE 68588-0299, USA

^d Department of Theoretical Chemistry, Jagiellonian University, 30-060 Krakow, Poland

^e Department of Chemistry, State University of New York at Buffalo, Buffalo, NY, 14260-3000, USA

[†] Electronic supplementary information (ESI) available. See DOI: 10.1039/c4cc03523b

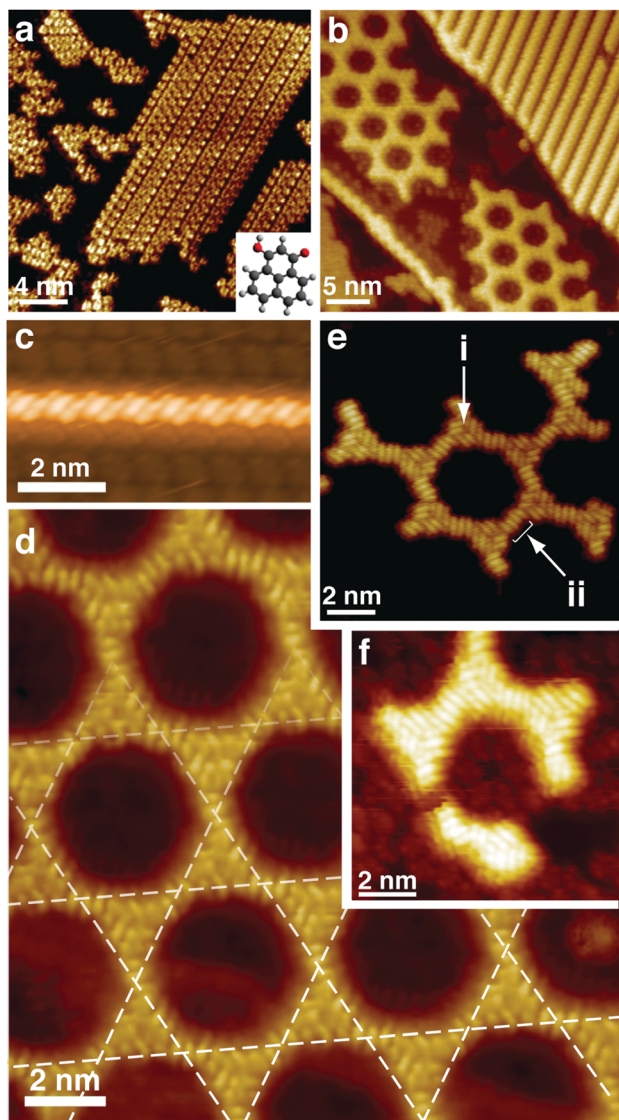


Fig. 1 Scanning tunneling microscopy images of 3-HPLN on Cu(111). (a) Sub-ML coverage after annealing to 120 °C. $I_T = 500$ pA, $V_b = -1$ V. Inset: 3-HPLN of form $C_{13}H_8O_2$; (b) approx. 2 ML of 3-HPLN, after annealing to 200 °C, $I_T = 500$ pA, $V_b = 1$ V; (c) linear chain in the second layer; $I_T = 600$ pA, $V_b = -0.3$ V; (d–f) images of honeycomb structures. Details highlighted in (e) are a trimer of dimers forming a junction (i) and a dimer of dimers forming a linear segment of the network (ii). The contrast in (f) has been adjusted to enhance the visibility of the first ML. Tunnel parameters in (d–f) are $I_T = 700$ pA, $V_b = 1$ V; $I_T = 500$ pA, $V_b = -0.6$ V; $I_T = 600$ pA, $V_b = -0.3$ V, respectively.

and also distinctively different from the annealed single layers in Fig. 1a. This leads us to conclude that the double layers have to be interpreted as a three-dimensional structure in which both layers form as one structure at the same time during the annealing, rather than merely being two layers added together.

Here we focus on the structure of the honeycomb-like layer, Fig. 1d–f. The symmetry of the lattice is reminiscent of a Kagome lattice, as is outlined by the interlacing triangles shown in Fig. 1d. It is noted that Kagome lattices create two types of voids and in the present structure one type of those

voids is extremely small. The hexagons and triangles are formed by the molecules in the top layer only. High-resolution STM images, including those taken on incomplete layers in (e and f) reveal important structural detail. The considerably smaller apparent size of the molecules in the second layer, as compared to those visible in the first layer, and their obvious arrangement into dimers, suggests that the molecules form π - π bonded dimers, which are then stacked into the honeycomb structure. Importantly, the top layer molecules are attached perpendicular to the flat-lying molecules underneath. Linear segments of two dimers (detail (ii) in Fig. 1e) are connected on both ends to chiral, pinwheel-like junctions consisting of three dimers (detail (i)). The chirality of the pinwheel junctions is the same for all junctions within a network, giving the symmetrized 2D network a six-fold rotation axis of symmetry (p6 wallpaper group) and overall space group chirality. Repeated film preparation has yielded both chiralities.

We have performed geometry optimization based upon density functional theory (DFT) calculations to explore the network architecture in greater detail, specifically the exact alignment of the molecules within the lattice. The computational models are described in the ESI.† The study of a unit cell of the entire double layer was computationally too expensive, and further hampered by the uncertainty in the structures of both the bottom and the top layer. We therefore limited our analyses to small free and supported model clusters, such as dimers, tetramers and hexamers, to investigate structural features of the top layer. The most stable clusters from the DFT calculations are summarized in Fig. 2, while other clusters considered and their relative energies are given in the ESI.† First, we established that the molecules in the most stable π - π stacked free dimer are aligned such that the carbonyl group of one molecule is in juxtaposition with the hydroxyl group of the other one. This alignment of the two 3-HPLN molecules results in tilted hydroxyl hydrogens towards the carbonyl oxygens, adding hydrogen bond character to the dominating intermolecular π - π stacking. The preferential stacking of two such dimers into a free 1D chain is such that the O- and OH-containing ends of neighboring dimers point in opposite direction (Fig. 2c). Interestingly, the lowest energy pinwheel junctions consist of three dimers that are different from the lowest energy free dimer in that the two molecules within a dimer are identically aligned (Fig. 2b). It appears that such an alignment enables a shared hydrogen bond between the two hydroxyl H's in one dimer and one carbonyl O of a neighboring dimer. Our calculations further show that the alternating dimer arrangement is no longer preferred upon attachment of two 3-HPLN dimers to a flat-lying layer of 3-HPLN on a Cu slab in a fashion seen in the STM image in Fig. 1c. Aligning all dimers with their functional groups towards the bottom layer (Fig. 2d) lowers the energy by 0.4 eV per molecule, as compared to the alternating dimer arrangement (Fig. S6 in ESI†).

While the bottom layer of the bilayers is mostly hidden by the top layer, STM images of incompletely assembled top layer structures such as those in Fig. 1f provide clues about the make-up of the bottom layer. Bottom layer molecules are visible inside the hexagonal pores of the Kagome lattice, and they

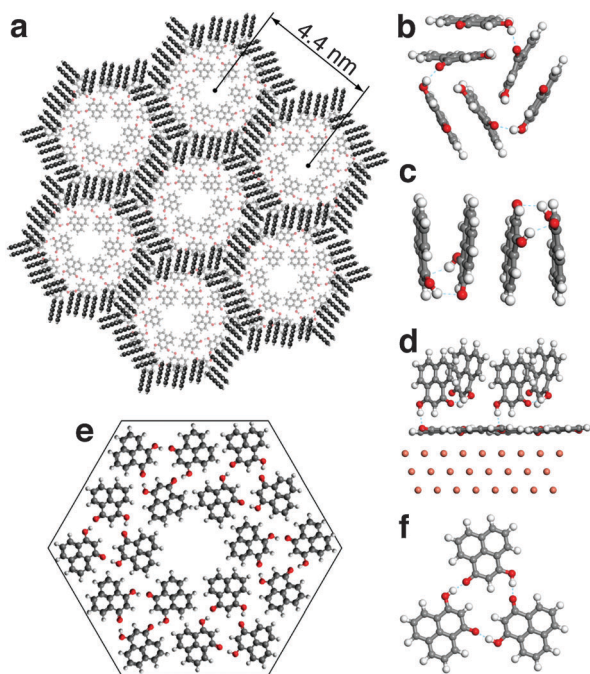


Fig. 2 (a) Model of the Kagome lattice of 3-HPLN on Cu(111). The model was constructed considering calculated lowest-energy clusters of molecules, such as (b) free hexamers, (c) free tetramers, (d) two supported dimers on flat-lying molecules and Cu(111) slab (side view). (e) Structure model of a hexagonal cell of the first layer of flat-lying molecules, as used in (a) with the lowest energy trimer in (f).

apparently arrange in a circular fashion within the exposed area, leaving a pore in the center. The analysis of several images taken near defects in the top layer reveals a remarkable similarity of the bottom layer with the chiral porous monolayers observed for 3-HPLN on another substrate, Ag(111).⁶ The fundamental building blocks of those networks on Ag(111) are planar trimers of 3-HPLN, which are arranged into a network with $(2\sqrt{13} \times 2\sqrt{13})R13.9^\circ$ epitaxial orientation to the substrate. The resulting pore-to-pore distance is 2.08 nm, which is considerably smaller than the 4.4 ± 0.2 nm measured for the present structures. Based on the structure information from this STM study and comparison to the networks of 3-HPLN on Ag(111) we developed the structure model of the bottom layer shown in Fig. 2a and e. It is also based on the most stable trimer of 3-HPLN, but their relative orientation is different compared to their arrangement on Ag(111), creating a larger unit cell. This model matches remarkably well with our experimental observations, resembling basic features and dimensions. However, it should be noted that this structure has never been observed with STM in monolayers of 3-HPLN on Cu(111), for any annealing temperature up to 240 °C. It is thus concluded that this porous layer of 3-HPLN might only be stable in a bilayer arrangement on Cu(111), whereas single layers always seem to prefer linear chain formation.

We did not consider metallation of the organics using substrate atoms or deprotonation of the 3-HPLN in our simulations. Metallation has been reported for several organic species on Cu(111), since Cu atoms become readily available on the surface at sufficiently high temperature.⁷ For instance, we reported the formation of a metal–organic coordination network of the structurally related

rhodizonic acid on Cu(111) after moderate annealing to approx. 90 °C,⁸ *i.e.* at lower annealing temperature than what we used in this study. An immediate indicator for metallation is the degradation of the substrate, *i.e.* jagged step edges and holes within the terraces,⁸ which we never observed for the 3-HPLN–Cu(111) system. Deprotonation of organics is also frequently observed on Cu(111). Deprotonation typically increases the reactivity of the organics, and reports from the literature often show deprotonation occurring simultaneously with metallation,^{7–9} in some instances catalyzed by the lattice gas of Cu atoms.¹⁰ The absence of any structural degradation in the Cu surface is a hint against metallation and deprotonation, and we note that metallation and deprotonation, if present, would mainly affect the bottom layer.

In conclusion, the outstanding feature of the self-assembled 3-HPLN Kagome lattices on Cu(111) is the double-layer structure where the molecules in the top layer form π – π stacked dimeric building blocks, which are attached perpendicular to the bottom layer. The bottom layer most likely consists of planar trimers of 3-HPLN, which we reported earlier. Importantly, this structure only exists in a bilayer, whereas single layers of 3-HPLN exhibit entirely different molecular arrangement. This dependence of the structure of both layers on each other means that the film structure is in fact three-dimensional. This remarkable feature distinguishes the present system from other layer-by-layer grown systems with perpendicular molecule attachment, such as terephthalic acid on Cu(100).¹² However, the combination of π – π stacking and perpendicular attachment is in striking analogy to the crystal structure of 3-HPLN in the bulk.¹¹ The discovered structure does not only represent a rare example of a three-dimensional arrangement of molecules on a two-dimensional surface, it involves molecules that exhibit ferroelectricity from hydrogen bond ordering in bulk crystals. Thus, this study potentially contributes to the emerging field of 2D organic ferroelectrics.

This work was supported by grants DMR-0820521 and EPS-1004094. Support from the Center of Computational Research at SUNY Buffalo and the Holland Computing Center at UNL is acknowledged. JH thanks the HOMING PLUS/2012-6/4 program, granted by the FNP and cofinanced by the EU. E.Z. thanks the Alfred P. Sloan Foundation for a research fellowship (2013–2015).

Notes and references

- (a) S. Furukawa, H. Uji-I, K. Tahara, T. Ichikawa, M. Sonoda, F. C. De Schryver, Y. Tobe and S. De Feyter, *J. Am. Chem. Soc.*, 2006, **128**, 3502; (b) Z. Shi and N. Lin, *J. Am. Chem. Soc.*, 2009, **131**, 5376; (c) T. Chen, Q. Chen, X. Zhang, D. Wang and L.-J. Wan, *J. Am. Chem. Soc.*, 2010, **132**, 5598; (d) U. Schlickum, R. Decker, F. Klappenberger, G. Zoppellarp, S. Klyatskaya, W. Auwärter, S. Neppel, K. Kern, H. Brune, M. Ruben and J. V. Barth, *J. Am. Chem. Soc.*, 2008, **130**, 11778; (e) H. Zhou, H. Dang, J.-H. Yi, A. Nanci, A. Rochefort and J. D. Wuest, *J. Am. Chem. Soc.*, 2007, **129**, 13774; (f) M. Blunt, X. Lin, M. d. C. Gimenez-Lopez, M. Schröder, N. R. Champness and P. H. Beton, *Chem. Commun.*, 2008, 2304.
- (a) D. G. Nocera, B. M. Bartlett, D. Grohol, D. Papoutsakis and M. P. Shores, *Chem. – Eur. J.*, 2004, **10**, 3850; (b) L. Messio, B. Bernu and C. Lhuillier, *Phys. Rev. Lett.*, 2012, **108**, 207204.
- J. T. Chalker and J. F. G. Eastmond, *Phys. Rev. B: Condens. Matter Mater. Phys.*, 1992, **46**, 14201.
- S. Horiuchi, R. Kumai and Y. Tokura, *Adv. Mater.*, 2011, **23**, 2098.

- 5 J. Hooper, D. A. Kunkel, S. Simpson, S. Beniwal, A. Enders and E. Zurek, *Surf. Sci.*, 2014, DOI: 10.1016/j.susc.2014.04.015.
- 6 D. A. Kunkel, J. Hooper, S. Simpson, G. A. Rojas, S. Ducharme, T. Usher, E. Zurek and A. Enders, *Phys. Rev. B: Condens. Matter Mater. Phys.*, 2013, **87**, 041402(R).
- 7 N. Lin, A. Dmitriev, J. Weckesser, J. V. Barth and K. Kern, *Angew. Chem., Int. Ed.*, 2002, **41**, 4779–4783.
- 8 D. A. Kunkel, J. Hooper, S. Simpson, S. Beniwal, K. L. Morrow, D. C. Smith, K. Cousins, S. Ducharme, E. Zurek and A. Enders, *J. Phys. Chem. Lett.*, 2013, **4**, 3413.
- 9 C. C. Perry, S. Haq, B. G. Frederick and N. V. Richardson, *Surf. Sci.*, 1998, **409**, 512–520.
- 10 M. N. Faraggi, C. Rogero, A. Arnau, M. Trelka, D. Écija, C. Isvoranu, J. Schnadt, C. Marti-Gastaldo, E. Coronado and J. M. Gallego, *et al.*, *J. Phys. Chem. C*, 2011, **115**, 21177–21182.
- 11 T. Mochida, S. Matsumiya, A. Izuoka, N. Sato, T. Sugawara and Y. Sugawara, *Acta Crystallogr., Sect. C: Cryst. Struct. Commun.*, 1992, **48**, 680–683.
- 12 S. L. Tait, H. Lim, A. Theertham and P. Seidelz, *Phys. Chem. Chem. Phys.*, 2012, **14**, 8217–8223.